Chapter 41
Integrated Renewable Energy-Based Systems for Reduced Greenhouse Gas Emissions

Mehdi Hosseini, Ibrahim Dincer, and Marc A. Rosen

Abstract Efforts to develop systems to mitigate environmental pollution are increasing. Renewable energy resources, e.g., solar, wind, and hydro, provide clean energy with almost no greenhouse gas emissions. However, these forms of energy are intermittent, and the costs of systems utilizing renewable energy for power generation or heating/cooling are often not competitive with conventional systems. Using hybrid systems and recovering waste energy are two ways to enhance the utilization of renewable energy resources. In this chapter, numerous integrated renewable-based energy systems are reviewed, based on a number of previous studies by the present authors. The aims of these systems are to enhance energy management and reduce environmental pollution. The chapter starts with a brief introduction of integrated renewable energy systems and their role in mitigating environmental pollution. The description of some integrated systems for residential and community usage is presented. Moreover, the systems are compared with conventional power generation systems in terms of efficiency and carbon dioxide emission. The results show that although the energy efficiency of the residential photovoltaic-fuel cell system is considerably lower than the conventional power generation systems, they release zero amount of emission into the environment during their operation. Fuel cell-micro gas turbine system integrated with biomass gasification has energy efficiencies around 55 %. This renewable-based energy integrated system produces 741 gram of carbon dioxide per kWh, which is comparable with the emission of fossil power plants.

M. Hosseini (✉) • I. Dincer • M.A. Rosen
Faculty of Engineering and Applied Science, University of Ontario Institute of Technology, 2000 Simcoe Street North, Oshawa, ON, Canada L1H 7K4
e-mail: mehdi.hosseini@uoit.ca; ibrahim.dincer@uoit.ca; marc.rosen@uoit.ca

I. Dincer et al. (eds.), *Causes, Impacts and Solutions to Global Warming*,
DOI 10.1007/978-1-4614-7588-0_41,

Nomenclature

ex	Specific exergy, kJ/kg
$\dot{E}x$	Exergy flow rate, kW
i	Current density, A/cm^2
$\dot{I}$	Exergy destruction rate, kW
LHV	Lower heating value, kJ/kg
$\dot{m}$	Mass flow rate, kg/s
n	Reaction coefficient
$\dot{n}$	Molar flow rate, kmol/s
N	Number of cells in the SOFC
$\dot{Q}$	Heat flow rate, kW
SC	Steam-to-carbon ratio
T	Temperature, °C
$\dot{W}$	Electric power, kW

Greek Letters

η	Energy efficiency %
ψ	Exergy efficiency %
γ	Specific heat ratio

Subscripts

0	Ambient or standard condition
a	Air
$cell$	SOFC cell
ex	Exergy
g	Gas
i	Species
mb	Moist biomass
MGT	Micro gas turbine
DH	District heating heat demand
p	Product gas
Q	Heat
s	Surface or steam
TIT	Turbine inlet temperature
WB	Wet biomass

Superscripts

*	Reference condition

Acronyms

HRSG	Heat recovery steam generator
MGT	Micro gas turbine
SOFC	Solid oxide fuel cell
PV	Photovoltaic
PV-FC	Photovoltaic-fuel cell

41.1 Introduction

Many feel that present-day production and use of energy threaten the environment in terms of global warming, mainly as a consequence of greenhouse gas (GHG) emissions, and depletion of energy resources. According to the Carbon Dioxide Information Analysis Center (CDIAC), half of the GHG emissions during the period of 1751 to 2008 were released into the environment after 1971 [1]. Figure 41.1 shows the trend in carbon dioxide emissions due to the burning of fossil fuels since 1950. More than 70 % of the emissions reported in Fig. 41.1 are due to the use of solid and liquid fossil fuels [1]. The trend towards increasing energy consumption will likely exacerbate such environmental problems.

Attention towards developing systems to mitigate these environmental problems is increasing. Improving the efficiency of energy systems usually requires reducing irreversibilities and waste exergy losses, as well as the use of less environmentally impacting alternative energy resources. The use of renewable energy resources in power generation is receiving much focus. Renewable energy resources, e.g., solar,

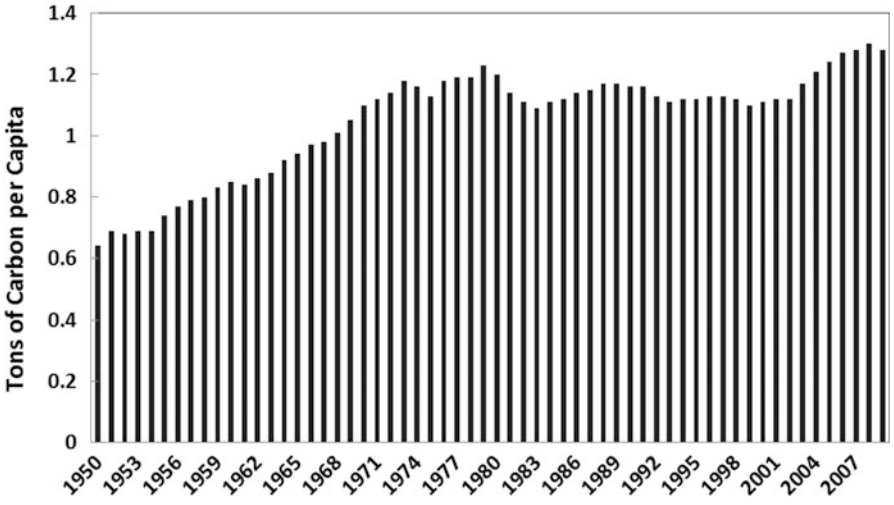

Fig. 41.1 Annual global fossil fuel carbon dioxide emissions per capita (modified from ref. 1)

wind, and hydro, provide clean energy with almost no GHG emissions. However, these forms of energy are intermittent, and the cost of systems utilizing renewable energy for power generation or heating/cooling is often not competitive with that of conventional systems. Using hybrid systems and recovering waste energy are two ways to enhance the utilization of renewable energy resources. Solar energy can be used for space heating/cooling and for electricity generation with photovoltaic (PV) systems. Such systems normally require supplementary devices to meet peak demands or to harvest surplus generated electricity. Producing the energy carrier hydrogen is one method for storing electricity from solar PV systems. Surplus electricity can be converted to hydrogen via water electrolysis, and the hydrogen can be stored and used to generate electricity, when required, in a fuel cell. The fuel cell also can cogenerate heat for district heating or other purposes. Biomass, another renewable energy resource, can be used directly (direct burning) or indirectly (as a biofuel) to generate electricity. Biomass gasification has been demonstrated to be a feasible and promising technology and may play an important role in future energy markets. The syngas produced by gasification can be used in internal combustion engines (ICEs), gas turbines (GTs), and fuel cells (FCs). A power generation system utilizing biomass gasification can be integrated with bottoming cycles for heat recovery to increase efficiency. Integrated renewable energy-based systems (IRESs) combine power generation technologies with heat recovery and energy storage technologies to provide cooling, heating, and energy storage using thermal energy normally wasted in the production of electricity. Since the input energy is provided by renewable resources, IRESs exhibit almost no GHG emissions.

The configuration of the IRES components is important to optimize energy utilization. These systems consist of electricity generation technologies, process equipment, heat recovery units, and energy storage systems. Several configurations and technologies have been investigated. For instance, a market assessment for integrated energy systems (IESs) for buildings by LeMar [2] shows that the potential building market for IESs is expected to exceed 35 GW by the year 2020.

The current work is a review based mainly on previous research by the authors on the integration of renewable energy resources in supplying the electricity demand of a house or a community [3–7]. The presented IRESs are aimed in large part at decreasing the level of GHG emissions and enhancing energy management.

41.2 Hybrid Solar-Fuel Cell CHP Systems for Residential Applications

Numerous studies have been undertaken to improve the understanding of residential applications of solar-hydrogen combined heat and power (CHP). Here we consider such a hybrid system and describe its components and compare it with

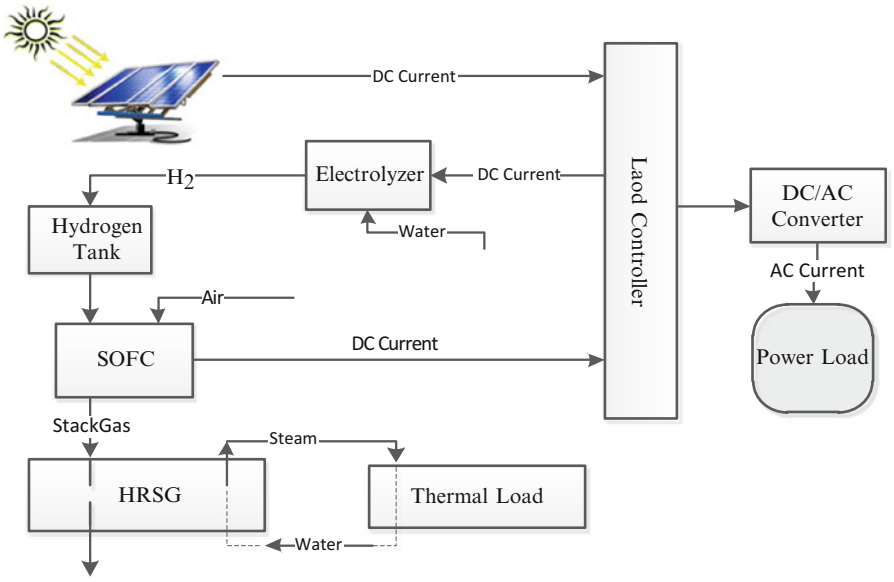

Fig. 41.2 Schematic of a photovoltaic-fuel cell CHP system for residential applications [4]

conventional CHP systems and solar-hydrogen CHP systems. The solar PV system is the main part of the electricity generation module. A proton exchange membrane (PEM) water electrolyzer is utilized for hydrogen production from surplus PV electricity. Hydrogen is stored during day when loads are below the peak and input into a solid oxide fuel cell (SOFC) to provide residential electricity at night. High-temperature gases leaving the fuel cell stack are directed to a heat recovery steam generator (HRSG), as shown in Fig. 41.2, for steam generation.

Gibson and Kelly [8] optimized a solar power hydrogen production system with water electrolysis. They showed that if all the components are selected and sized in an optimized way, so that the PV output voltage matches the electrolyzer input voltage, the overall solar-PV-hydrogen production system efficiency can reach 12.4 %. Lagorse et al. [9] investigated three PV-hydrogen production configurations for residential applications focusing on optimum size, cost, and operation. Pregger et al. [10] discussed four hydrogen production systems using solar thermal energy and performed cost evaluations.

The power output of the PV system depends strongly on the solar irradiance, as shown in Fig. 41.3 for a 210 W SunPower solar panel.

The intermittent and variable intensity solar irradiance affects the performance of the hybrid system. However, with appropriate design and using energy storage, the electricity demand of the house and a part of its thermal energy demand can be met. The surplus electricity generated by the PV modules is stored as hydrogen in a compressed hydrogen tank. Hydrogen can be stored as a liquid at cryogenic temperatures in relatively small volumes. The hydrogen liquefaction process

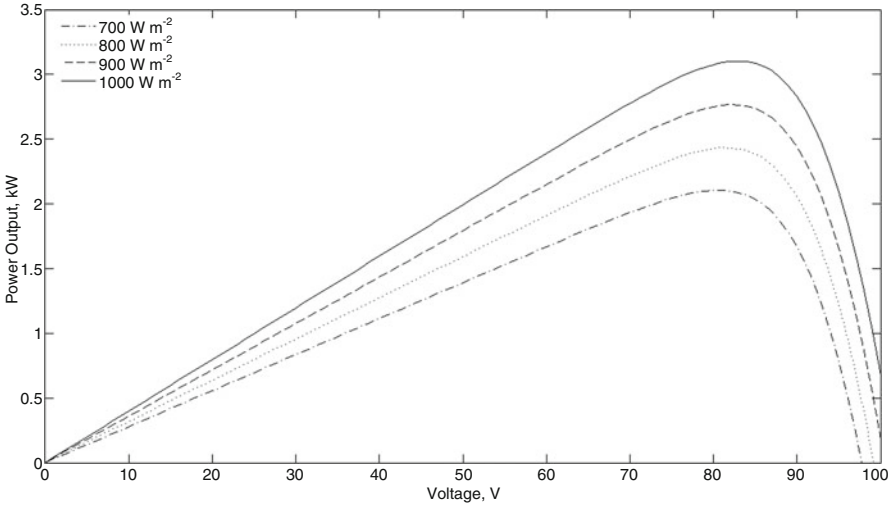

Fig. 41.3 Effect of solar irradiance on PV power-voltage characteristics

normally consumes more than 30 % of the hydrogen lower heating value (LHV) [7]. Hydrogen can also be stored as a compressed gas in pressure vessels, and via metal hydrides. In residential applications, especially when fuel cells are used in solar-fuel cell hybrid systems, large-scale hydrogen storage is not needed, so compressed gas hydrogen storage is usually preferred. During the storage of hydrogen as a compressed gas some physical exergy is lost due to pressure and temperature drops. The storage tank state of charge (SOC) and the pressure and temperature distribution depend on the tank filling rate, initial SOC, and pressure. The authors report the thermodynamic evaluation of filling a high-pressure storage tank [7]. At the tank initial temperature, the initial pressure has a positive effect on the exergy efficiency during filling. The exergy efficiency of the filling process rises from 86 to 89 % with an increase of initial tank pressure from 0.2 to 20 bar at the 20 °C initial temperature [7].

Fuel cells can be used for electricity generation, although technical and economic enhancements are still needed. They can also be used for CHP, and in hybrid configurations. Micro gas turbine-fuel cell (MGT-FC), MGT-steam turbine-FC, and MGT-FC district heating and cooling systems are operating in different regions of the world. For instance, Hosseini et al. [11] performed energy and exergy analyses for a residential hybrid MGT-FC system, and other works have been reported on residential fuel cell applications [12, 13]. Velumani et al. [14] proposed a hybrid SOFC/micro gas turbine/absorption chiller to provide electricity and cooling for a residential area, while Hartkopf et al. [15] investigated fuel cell use for a multipurpose building in the United States.

The exergy efficiency, which is an index of efficiency of the hybrid PV-fuel cell system relative to an ideal version of such a system, is presented based on the solar irradiance in Toronto and the electricity demand of a Canadian house. Figure 41.4

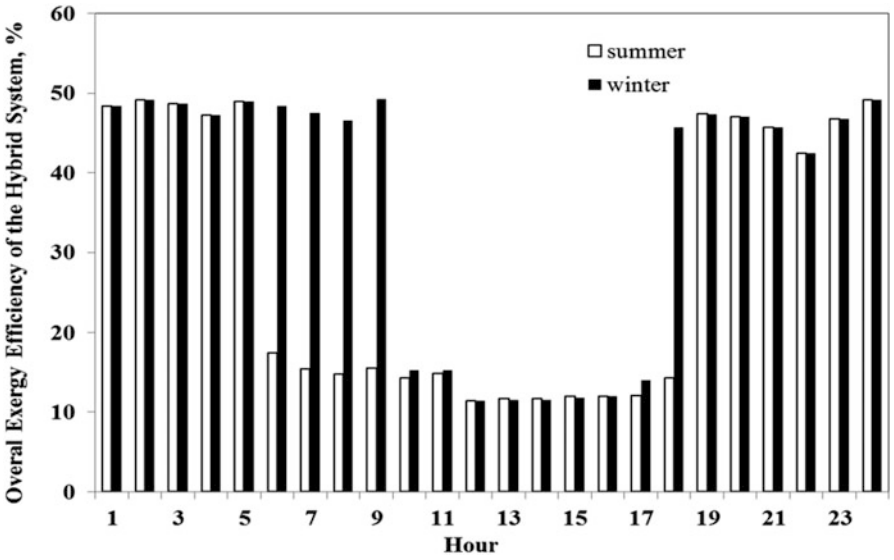

Fig. 41.4 Total exergy efficiency of a solar PV-FC CHP system broken down by hour of the day [4]

shows the exergy efficiency during two typical summer and winter days as a comparison. The efficiency graph shows that the time that the fuel cell is in operation is longer in winter. This is mostly due to less solar availability in winter. The minimum total efficiency is achieved when the surplus electricity generation is a maximum. In summer, the system exhibits a minimum total exergy efficiency between 6 am and 6 pm, because the surplus power generated by the PV system is consumed in the electrolyzer for hydrogen production. This minimum efficiency operation period for winter is from 10 am to 5 pm.

41.2.1 Comparison of Conventional and Solar-Hydrogen Residential CHP Systems

Fuel cells and solar PV systems are both undergoing extensive development, and their uses in industrial and residential applications are presently limited. Several CHP systems (e.g., micro gas turbines, internal combustion engines, and diesel generators) are being used to provide electricity and heating/cooling for houses. It is possible for these systems to operate independently of the power grid. These systems also allow heat recovery from the system flue gas. For both conventional and solar-fuel cell CHP systems, reliability, control, economics, and emissions are major concerns.

Table 41.1 Electrical and thermal power outputs and efficiencies for several CHP systems

	Product power output (kW)		Energy efficiency (%)	
CHP system	Electrical	Thermal	Electrical	Thermal
Gas engine	5.5	12.5	27	61
Internal combustion engine	2.0–9.5	8.0–26	24	72
Fuel cell	4.0	9.0	25	55
PV-fuel cell	3.6	0.50	–	14.5

Source: Ref. 4

Table 41.2 Energy efficiency and specific CO_2 emissions for several electricity generation plants

Electricity generation plant	Energy efficiency (%)	Specific CO_2 emission (g/kWh)	Reference
Combined cycle power plant	50	404	[16]
Fossil fuel power plant	42	617	[16]
Nuclear power plant and conventional steam power plant	37	272	[16]
Residential PV-fuel cell	14.5	0	[4]

The results of a comparative analysis based on selected micro-CHP technologies for residential applications are shown in Table 41.1. The nominal power and the energy efficiency during the maximum load are considered in the analysis, which are adapted from the work by Paepe et al. [16]. Table 41.1 shows the electrical and thermal power outputs and energy efficiencies of the selected CHP systems.

Every electricity and heat generation system has emissions, the magnitude of which depends on system type. Paepe et al. [16] predicted that, if the heat is generated by a gas boiler, the specific CO_2 emission is 404 g/kWh of natural gas combusted. The CO_2 produced through electricity generation is strongly dependent on the electricity generation technology and its efficiency. Table 41.2 shows the energy efficiency and CO_2 emissions for the three electricity generation methods operating in Belgium. Also, the results for a residential PV-FC CHP system are presented.

To compare the CHP systems with the power generation technologies in Table 41.2, the same procedure is used to determine the CO_2 emissions. Since the gas engine and the Stirling internal combustion engine use natural gas, the specific CO_2 emission is considered to be 56.1 g per 1 MJ natural gas consumption. For the fuel cells, it is assumed that no CO_2 is produced during operation. However, CO_2 is produced during the production of the H_2 for the fuel cells (from the methane-reforming reaction if natural gas is the fuel). The efficiency of the reforming reaction is taken into account in the efficiency of the fuel cell. Assuming that natural gas is used to produce the hydrogen in the fuel cell, one can consider 56.1 g/MJ as applicable to the fuel cell, too.

In the next step, Paepe et al. [16] simulated the electrical and thermal demands of a house in Belgium, and determined the annual electricity demand to be 3.61 MWh and the annual thermal load to be 34.19 MWh. The energy consumption for the

Table 41.3 Fraction of energy consumption for several CHP systems relative to several conventional power generation systems

	Type of power generation system		
CHP system	Combined cycle	Fossil fuel	Nuclear and conventional steam
Fuel cell	0.87	0.79	0.70
Gas engine	0.81	0.71	0.64
Internal combustion engine	0.73	0.65	0.59

three CHP systems and the cases in which electricity is supplied by a power grid are compared in Table 41.4, where values are relative to the reference cases: a gas-fired combined power plant, a fossil fuel power plant, and a nuclear power plant and conventional steam power plant. Table 41.3 demonstrates that the internal combustion engine has the greatest energy saving compared to the conventional power generation systems. Compared to the nuclear power plant, the internal combustion engine CHP systems reduce energy consumption the most. All three CHP systems have lower emissions than the fossil fuel power plant. Energy use and CO_2 emission reductions strongly depend on the power plant efficiency. Since the energy efficiency of the fuel cell CHP system is less than that of other CHP systems, its energy saving fraction is also less [16].

Although the PV-fuel cell system for the residential applications produces zero GHG emissions during operation, emissions occur during manufacturing of the system components. A detailed life cycle analysis is required to assess residential CHP systems in terms of resource consumption and environmental pollution during the manufacturing processes. Nonetheless, with improving manufacturing processes, implementing a renewable-based integrated system to power a residential area will likely help in sustaining the environment.

41.3 Integrating a Solid-Oxide Fuel Cell and Micro Gas Turbine with Biomass Gasification

Gasification is a chemical process that converts materials such as biomass into convenient gaseous fuels. In this process biomass is broken into simpler substances like CO, H_2, CH_4, and CO_2. The process occurs in the presence of a gasification medium [17–19]. Biomass gasification is a complicated process, which is affected by many parameters, including gasification medium, biomass composition and moisture content, gasification temperature and pressure, and process configuration. A good understanding of the effects of these parameters on the performance of a gasification system is required for effective design [5]. Thermodynamic analysis, based on exergy as well as energy, is one approach to develop such an understanding. Various studies have been performed on biomass gasification from the point of energy and exergy. For example, Cohce et al. [17] analyzed a hydrogen production

unit based on biomass gasification; a simplified model is presented for biomass gasification based on chemical equilibrium considerations, with the Gibbs free energy minimization approach, hydrogen production and exergy destruction rates in each component are found. Abuadala et al. [18] presented an exergy analysis of a hydrogen production system via biomass gasification in the range of 10–32 kg/s from sawdust. The study focuses on the influence of gasification temperature, biomass feed, and steam injection on the hydrogen yield and energy efficiencies. The results indicate that the performance of hydrogen production from steam-fed biomass gasification depends on the quantities of steam and biomass input to the gasifier.

The product gas mixture for biomass gasification contains several species, depending on the process type and operational conditions. Stoichiometric calculations can help determine the products of reaction [19]. Abudallah and Dincer [20] considered the use of biomass gasification product gas as the fuel feed to an SOFC, as a potential integrated application. The current authors consider a similar system in which the product gas is fed to the fuel cell stack after gas cleaning and CO_2 removal [6].

The integrated system includes a biomass gasification unit, an SOFC, a micro gas turbine, and a heat recovery unit (see Fig. 41.5). Sawdust is fed to the biomass dryer before entering the gasifier. In the analyses, a direct-steam drying process is considered to remove 50 % of the biomass moisture content. In the gasifier, biomass is converted to a mixture of gases in the presence of superheated steam. Biomass gasification is an endothermic process, and the gasification system is considered to be indirectly heated by an external heat source.

The product gas mixture leaving the gasifier contains CO, H_2, CH_4, CO_2, H_2O, N_2, and C. The LHV of the product gas is highly dependent on the mixture composition. Moreover, downstream components in the integrated system are affected by the gas properties. Therefore, gas cleaning and CO_2 removal are added to the system. With these post-gasification processes, the product syngas consists of CO, H_2, and CH_4 and is fed to the solid oxide fuel cell for power production.

The basic electrochemical reactions taking place in an SOFC stack are given by [21, 22]

$$CH_4 + H_2O \leftrightarrow 3H_2 + CO \tag{41.1}$$

$$CO + H_2O \leftrightarrow H_2 + CO_2 \tag{41.2}$$

$$2H_2 + O_2 \rightarrow 2H_2O \tag{41.3}$$

Characteristic curves of SOFCs are obtained based on the equilibrium constants and reaction rates of Eqs. 41.1–41.3. The oxygen ions are formed in the cathode side of the fuel cell and pass through the electrolyte to the anode. The electrochemical reaction of hydrogen and oxygen ions releases electrons, which pass through an external electric circuit providing the power output of the SOFC. To avoid cell

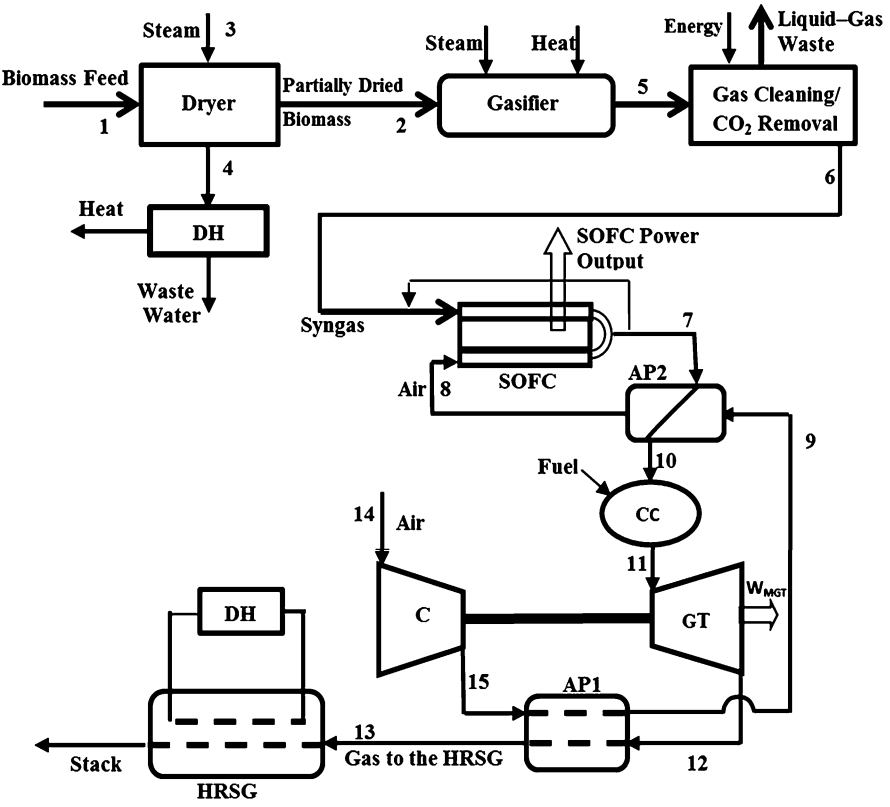

Fig. 41.5 Schematic of the integrated SOFC-micro gas turbine with biomass gasification

starvation, only a certain percent of the syngas reacts with oxygen ions in the anode. This is specified by a fuel utilization factor. The by-product gas of the electrochemical reactions leaves the fuel cell stack with a temperature between 800 and 1,000 °C. Also, the by-product contains some non-reacted syngas. In order to recover the energy from the SOFC exhaust gas, an afterburner is utilized to burn the remaining syngas and provide the micro gas turbine with the required input energy. Therefore, the by-product gas leaving the fuel cell anode side mixes with the air from the cathode side. The combustion process in the afterburner produces a high-enthalpy gas which can be used in the MGT for electric power generation. Before the combustion gas enters the micro gas turbine, it is utilized to preheat the air entering the fuel cell stack. The combustion chamber of the micro gas turbine is used to fix the turbine inlet temperature (TIT). The combustion gases enter the MGT, produce mechanical energy, and leave the MGT with a temperature between 550 and 750 °C, depending on the compressor pressure ratio. The mechanical energy of the MGT is converted to electricity in the generator. The MGT flue gas has a significant amount of energy, which is recovered in the heat recovery steam

generator. The flue gas enters the HRSG and transfers its energy to the water flowing inside the tubes of the HRSG. Unless applied for power generation purposes, most HRSGs produce saturated steam for steam-utilizing units.

Superheated steam is used as the gasification medium in the gasifier. Sawdust is gasified in the presence of steam according to the following overall chemical equation:

$$\mathrm{C_aH_bO_cN_d} + SC \times \mathrm{H_2O(steam)} + \dot{Q}_{\mathrm{gasifier}}$$

$$\rightarrow n_1\mathrm{CO} + n_2\mathrm{H_2} + n_3\mathrm{CH_4} + n_4\mathrm{CO_2} + n_5\mathrm{H_2O} + n_6\mathrm{N_2} + n_7\mathrm{C} \tag{41.4}$$

Minimization of the Gibbs free energy or the equilibrium reaction rate approach is used to obtain the reaction coefficients (n_1 to n_7) [5, 19].

The biomass dryer and district heating unit are parts of the gasification system. The energy and exergy balances, which permit the calculation of the steam input to the dryer and heat flow rate of the district heating unit, are presented by the authors elsewhere [5]. Considering these two components, the total energy and exergy efficiencies, respectively, of the gasification system can be obtained:

$$\eta_{\mathrm{gasification}} = \frac{\dot{m}_{\mathrm{syngas}} \times LHV_{\mathrm{syngas}} + \dot{Q}_{\mathrm{DH}}}{\dot{m}_{\mathrm{biomass}} \times LHV_{\mathrm{biomass}} + \dot{E}n_{\mathrm{Steam}} + \dot{Q}_{\mathrm{gasifier}} + \dot{E}n_{\mathrm{gas-cleaning}}} \tag{41.5}$$

$$\psi_{\mathrm{gasification}} = \frac{\dot{m}_{\mathrm{syngas}} \times ex_{\mathrm{syngas}} + \dot{E}x_{\mathrm{q,DH}}}{\dot{m}_{\mathrm{biomass}} \times ex_{\mathrm{biomass}} + \dot{E}x_{\mathrm{Steam}} + \dot{E}x_{\mathrm{Q}} + \dot{E}x_{\mathrm{gas-cleaning}}} \tag{41.6}$$

Here, steam use is considered for both the dryer and the gasifier.

Colpan et al. [22] developed a model for the electrochemical reaction in an SOFC. Their model considers a mixture of H_2, CO, and CH_4 as the syngas fuel.

The electric power output of the fuel cell stack can be expressed as

$$\dot{W}_{\mathrm{SOFC}} = V \times i \times A_{\mathrm{cell}} \times N_{\mathrm{SOFC}} \tag{41.7}$$

where V denotes the output voltage, i the current density, A_{cell} the single cell active area, and N_{SOFC} the total number of cells in the stack.

The modeling of the afterburner and the combustion chamber is based on combustion reactions of the remaining syngas in the fuel cell exhaust and the gas TIT. The gas turbine and the compressor are modeled based on isentropic relations and isentropic efficiencies. The gases leaving the MGT are fed to the HRSG to produce steam for steam/hot water utilization purposes. Accounting for the heat recovered in the HRSG, the total efficiencies of the SOFC-MGT CHP system are

$$\eta_{\mathrm{SOFC-MGT\ CHP}} = \frac{\dot{W}_{\mathrm{SOFC}} + \dot{W}_{\mathrm{MGT}} + \dot{Q}_{\mathrm{HRSG}}}{\dot{m}_{\mathrm{fuel,SOFC-MGT}} \cdot \mathrm{LHV_{syngas}}} \tag{41.8}$$

Table 41.4 Input parameters for the gasification system

Parameter	Value
Dryer	
Biomass feed rate (kg/s)	0.011
Superheated steam pressure (bar)	3
Superheated steam temperature (°C)	200
Moisture fraction of feed biomass ($kg_{moisture}/kg_{WB}$)	0.5
Gasifier	
Steam pressure (bar)	10
Steam temperature (°C)	400

Table 41.5 Input parameters for the SOFC system

Parameter	Value
Stack outlet temperature (°C)	1,000
Activation area (cm^2)	834
Cell current density (A/cm^2)	0.35
Fuel utilization factor	0.85
Compressor pressure ratio, r_c	9
AP1 outlet temperature (Point 9 in Fig. 41.1) (°C)	527

$$\psi_{\text{SOFC-MGT CHP}} = \frac{\dot{W}_{\text{SOFC}} + \dot{W}_{\text{MGT}} + \dot{E}x_{\text{Q,HRSG}}}{\dot{m}_{\text{fuel,SOFC-MGT}} \cdot ex_{\text{syngas}}} \tag{41.9}$$

The aim is to improve the understanding of integrated system performance, and this is accomplished by performing a parametric study of the effect of steam-to-carbon (SC) ratio on the performance of the SOFC-micro gas turbine (SOFC-MGT) cycle integrating biomass gasification. The variations in molar fraction and LHV of the syngas, and the gasification process exergy destruction and energy and exergy efficiencies, are reported, as SC changes.

The following assumptions are made in the analyses of the integrated SOFC-MGT system with biomass gasification [6]:

- The system operates at steady state.
- All gases are ideal.
- Heat losses to the environment from the system boundary are negligible.
- Pressure drops along the system are negligible.
- Gasification takes place in equilibrium.
- The sawdust biomass has a chemical formula $C_{4.643}H_{6.019}O_{2.368}N_{0.021}$.

Tables 41.4–41.6 list the input parameters for the analyses of the integrated system.

The effect of steam-to-carbon ratio on the syngas species molar fraction is shown in Fig. 41.6. When SC varies from 1 to 4.5, the hydrogen molar fraction increases 17.8 %, while the carbon monoxide and methane molar fractions decrease by 42.5 and 87.7 %, respectively. These significant changes in the molar fraction result in the variation of the total mass flow rate of the syngas with SC shown in Fig. 41.7. At SC = 2, the syngas mass flow rate reaches its maximum value, after

Table 41.6 Input parameters for the MGT-HRSG system

Parameter	Value
Micro gas turbine	
MGT isentropic efficiency	0.93
Turbine inlet temperature (K)	1,400
Heat recovery steam generator	
Pinch point temperature difference (°C)	10
Outlet steam pressure (bar)	10

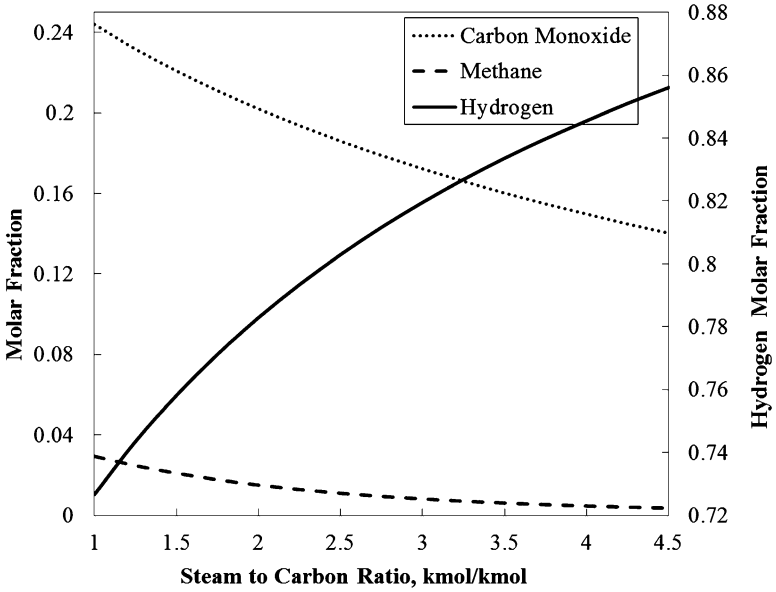

Fig. 41.6 Variation of molar fractions of syngas species with steam-to-carbon ratio

which it reduces gradually. The LHV of the syngas is calculated based on the molar fraction of each species in the mixture. The trade-off between the variations of molar fractions with the SC results in the final variation of LHV and is illustrated in Fig. 41.7.

The gasification heat requirement and exergy destruction rate are affected by the steam-to-carbon ratio. Introducing more steam to the gasifier decreases the need for external heat for the gasification process. The steam acts as the gasification medium and its energy content is used by the gasification process. With more steam entering the gasifier, more energy is introduced and the required heat input decreases.

According to Fig. 41.8, increasing the gasification temperature results in an increase in the heat requirement of the gasifier. Although, the heat requirement of the gasifier varies significantly with the change in temperature, the gasification process exergy destruction rate does not seem to be affected noticeably. This is seen in Fig. 41.9, where the exergy destruction rate is observed to decrease with increasing steam-to-carbon ratio.

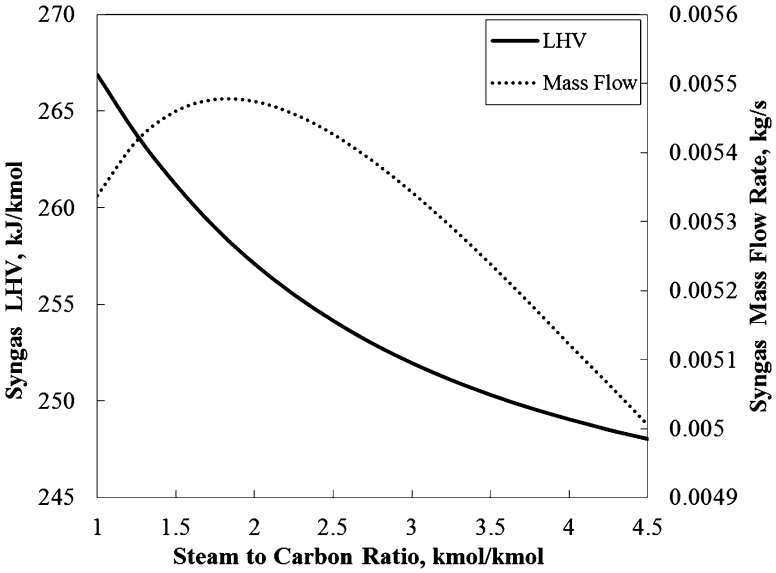

Fig. 41.7 Variation of syngas lower heating value and mass flow rate with steam-to-carbon ratio

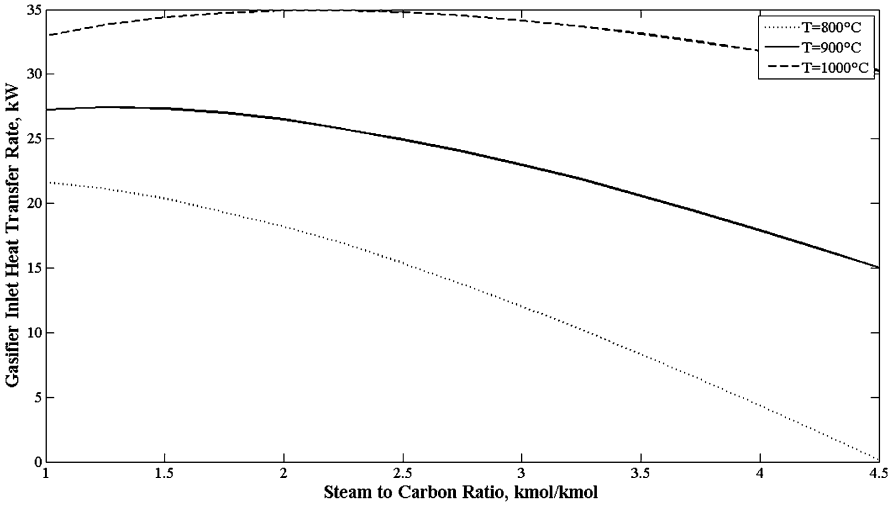

Fig. 41.8 Effect of steam-to-carbon ratio on gasifier heat requirement rate for various gasification temperatures

Energy and exergy efficiencies of biomass gasification are obtained using Eqs. 41.5 and 41.6. The variations of these efficiencies with SC and the gasifier temperature are illustrated in Figs. 41.10 and 41.11, respectively.

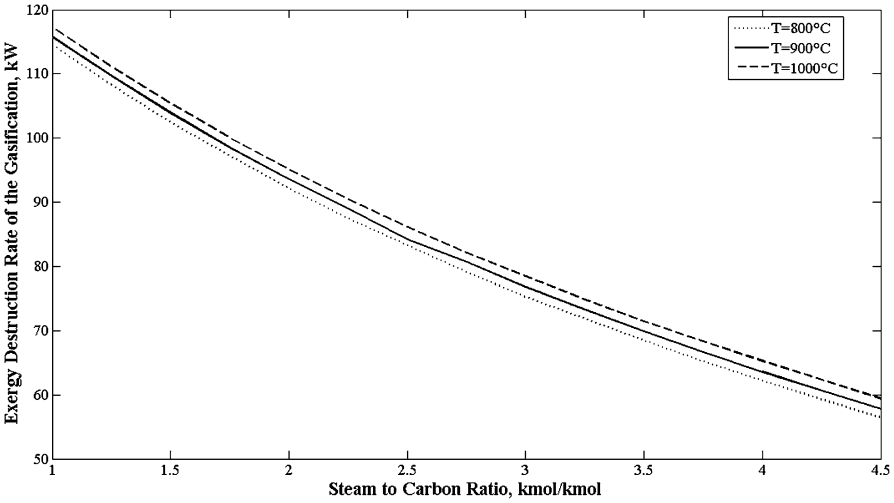

Fig. 41.9 Gasification exergy destruction rate vs. steam-to-carbon ratio for various gasifier temperatures

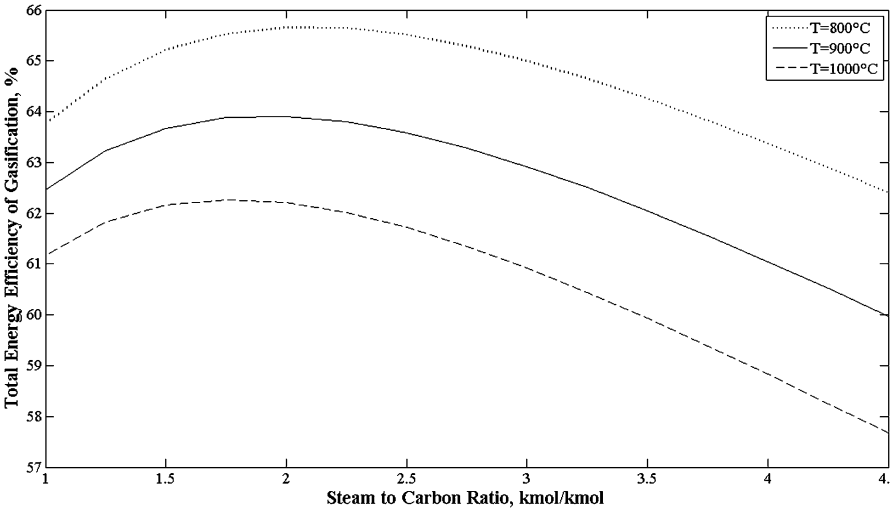

Fig. 41.10 Total energy efficiency of sawdust gasification vs. steam-to-carbon ratio, for various gasifier temperatures

Figure 41.6 shows that, for a gasifier temperature of 800 °C, the total energy efficiency of the gasification process reaches its maximum value of 65.6 % at SC = 2. With further increases in the temperature of the gasification medium into the gasifier, the energy efficiency drops, reaching 62.4 % for SC = 4.5. Increasing the gasification temperature reduces the total energy efficiency, as

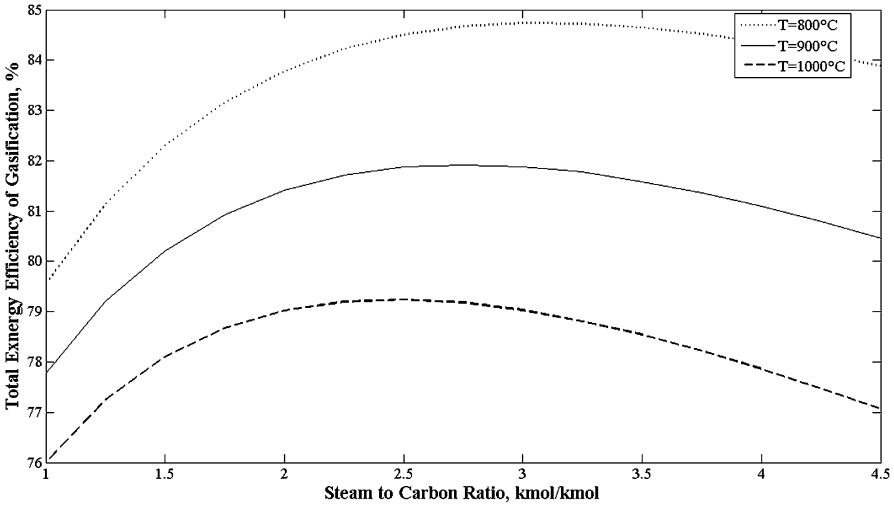

Fig. 41.11 Total exergy efficiency of sawdust gasification vs. steam-to-carbon ratio, for various gasifier temperatures

seen in Fig. 41.10. The gasification exergy efficiency exhibits a similar trend as the energy efficiency. However, the maximum value occurs at higher SC values. Higher values are achieved for efficiencies based on exergy compared to energy, because the exergy of heat is less than its energy. Since heat is an input to the gasification process, the denominator of the efficiency definition for exergy is less than that for energy.

The SOFC-MGT power output varies as a result of the change in the syngas LHV, as do the total energy and exergy efficiencies of the integrated SOFC-MGT system with biomass gasification. These variations are illustrated in Figs. 41.12 and 41.13.

According to the results in Fig. 41.3, the molar fraction of both CO and CH_4 decrease with increasing steam-to-carbon ratio. These two constituents are the source of CO_2 production in the SOFC-MGT cycle. However, by introducing more steam into the gasifier, the rate of CO_2 production increases, which results in an overall increase in the CO_2 emission of the integrated SOFC-MGT cycle with biomass gasification (Fig. 41.14).

Figure 41.14 can also be interpreted based on the extent of carbon dioxide emission per unit of electricity generation. For SC = 2, the hybrid SOFC-MGT system generates 87.7 kW net electricity power. Figure 41.11 shows that the CO_2 emission is 0.065 ton/h, which corresponds to 741 g/kWh. This compares well with the CO_2 emission levels of conventional power generation plants (Table 41.2). Moreover, since the biomass can be obtained in more sustainable ways, the carbon emissions of the biomass integrated system are less than the nonrenewable-based power generation systems.

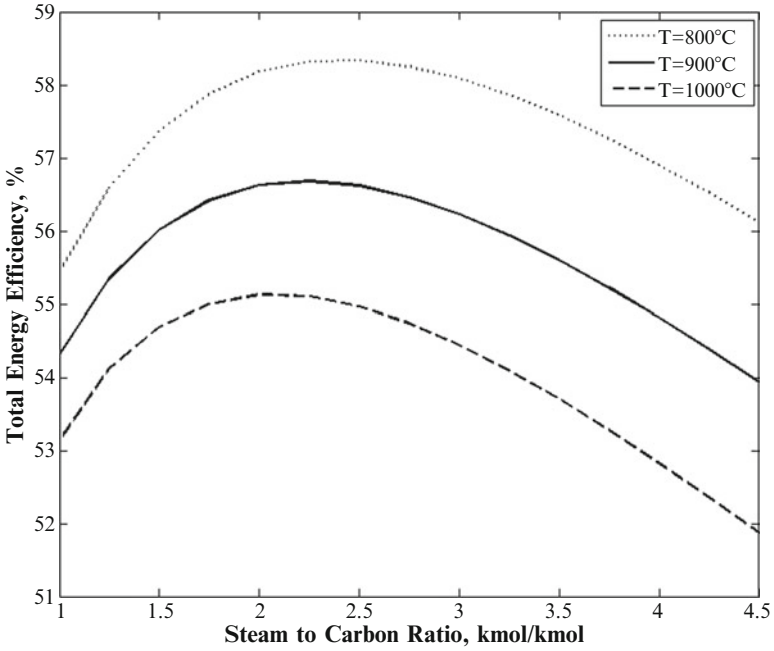

Fig. 41.12 Variation of total energy efficiency with SC for gasifier at various temperatures

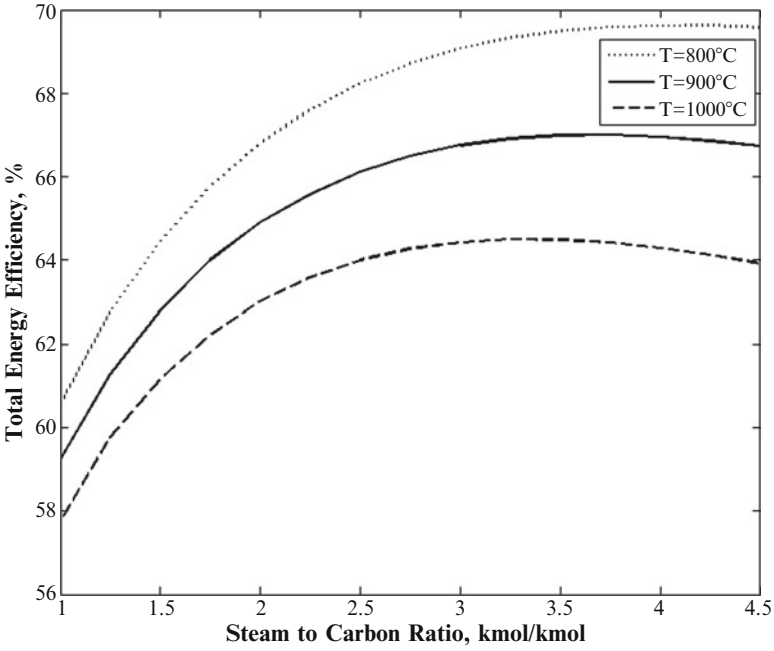

Fig. 41.13 Variation of total exergy efficiency with SC for gasifier at various temperatures

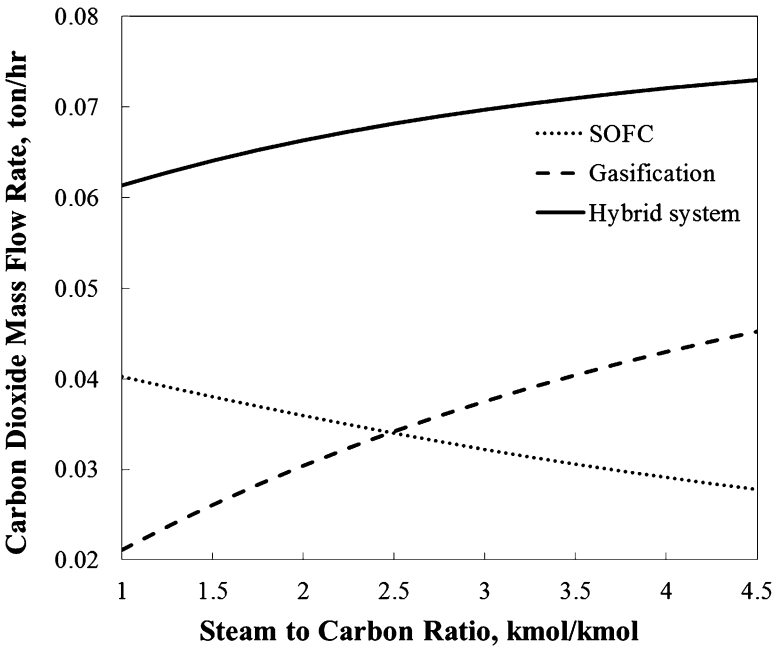

Fig. 41.14 Variation of carbon dioxide emission with steam-to-carbon ratio

41.4 Brief Review of Some Renewable-Based Energy Integrated Systems

Integrated renewable-based energy systems are not limited to the two systems presented above. Other sources of renewable energy can be used to exploit their clean and sustainable characteristics. For example wind energy can be added to the systems above, especially in coastal areas where there is a continuous (but variable) wind. Geothermal heat pumps are able to supply a portion (albeit small) of the thermal demand of a house or a district. Alternatively, they can be used to preheat the heating medium to reduce fuel consumption and GHG emissions. Syed et al. [23] studied the effect of an integrated, residential solar PV-wind turbine system on energy conservation and decreasing GHG emissions. They considered the use of PV and wind power in supplying a part of electricity demand of some Canadian houses. Depending on house type and location, hot water and space heating may be provided by electric heating or a natural gas furnace. The integrated renewable energy system is capable of generating a great portion of the house's electricity demand, which leads to a significant decrease in the GHG reduction. Syed et al. [23] reported that the national Canadian GHG reduction can be decreased by 4.1–12.7 Mton/year. Thus, this approach in which a Canadian house

is equipped with such a technology can be a significant step toward achieving sustainability in Canada, in terms of environmental stewardship.

In another example of IRESs, Calderon et al. [24] analyzed the components of an actual test-bed hybrid photovoltaic-wind system with hydrogen storage, in terms of energy and exergy. The test-bed is installed in the School of Industrial Engineering at the University of Extremadura, Spain. The system component irreversibility rates and exergy efficiencies are reported. The exergy efficiencies are as follows: electrolyzer: 68 %, photovoltaic module: 8.39 %, and fuel cell: 35.9 %. The authors concluded that designing more efficient PV modules can increase the utilization of the solar renewable energy, leading to less GHG emissions, when electricity is generated by solar and wind rather than fossil fuels.

The intermittency behavior of renewable energy resources can be addressed in part by energy storage. Greenblatt et al. [25] investigated the competition between gas turbines and compressed air energy storage (CAES) systems for integration with a base-load wind turbine.

They aim to explore the economic feasibility of using gas turbines to avoid problems associated with the intermittency of wind energy. In one strategy they suggest the integration of the wind turbine(s) with a gas turbine cycle. The gas turbine covers the load during periods when wind energy cannot meet the demand. Energy storage is another strategy to be integrated with the wind turbine(s). Since CAES is economically viable in terms of large-capacity storage of energy, Greenblatt et al. suggest its integration with wind energy systems. The wind power output is fed to an electric motor, which is connected to the air compressor of the CAES system (see Fig. 41.15).

The DC power generated by the wind turbines is consumed by the electric motor that is connected to the air compressor, which compresses ambient air to an intermediate pressure. Medium-pressure, high-temperature air releases its heat to a coolant in the intercooler and undergoes another compression process in the booster compressor. The work input to the booster compressor is provided by the wind turbines or by the power grid. High-temperature, compressed air releases its thermal energy to a cooling medium in the aftercooler and is stored in underground caverns. Whenever high-quality electricity is required by the power grid, the high-pressure stored air is extracted from the CAES system, and fed to the combustion chamber (CC) of the gas turbine, in which compressed air is heated by the combustion of natural gas or syngas.

According to Calderon et al. [24] the estimated electrical round-trip efficiency would be in the range of 77–89 %. They also estimate the cost of electricity (COE) for different systems and the effect of the natural gas price. The optimal COE using the wind-CAES system is 6.5 ¢/kWh for case in which the natural gas price is $9.0/GJ. For lesser prices of natural gas, combined cycle power plants exhibit the minimum cost of electricity generated. However, the primary advantage of the renewable wind-CAES system is the reduction in GHG emissions. With only 32 g/kWh CO_2 emissions, the wind-CAES system emits one-fourth of the emissions from a natural gas combined power plants.

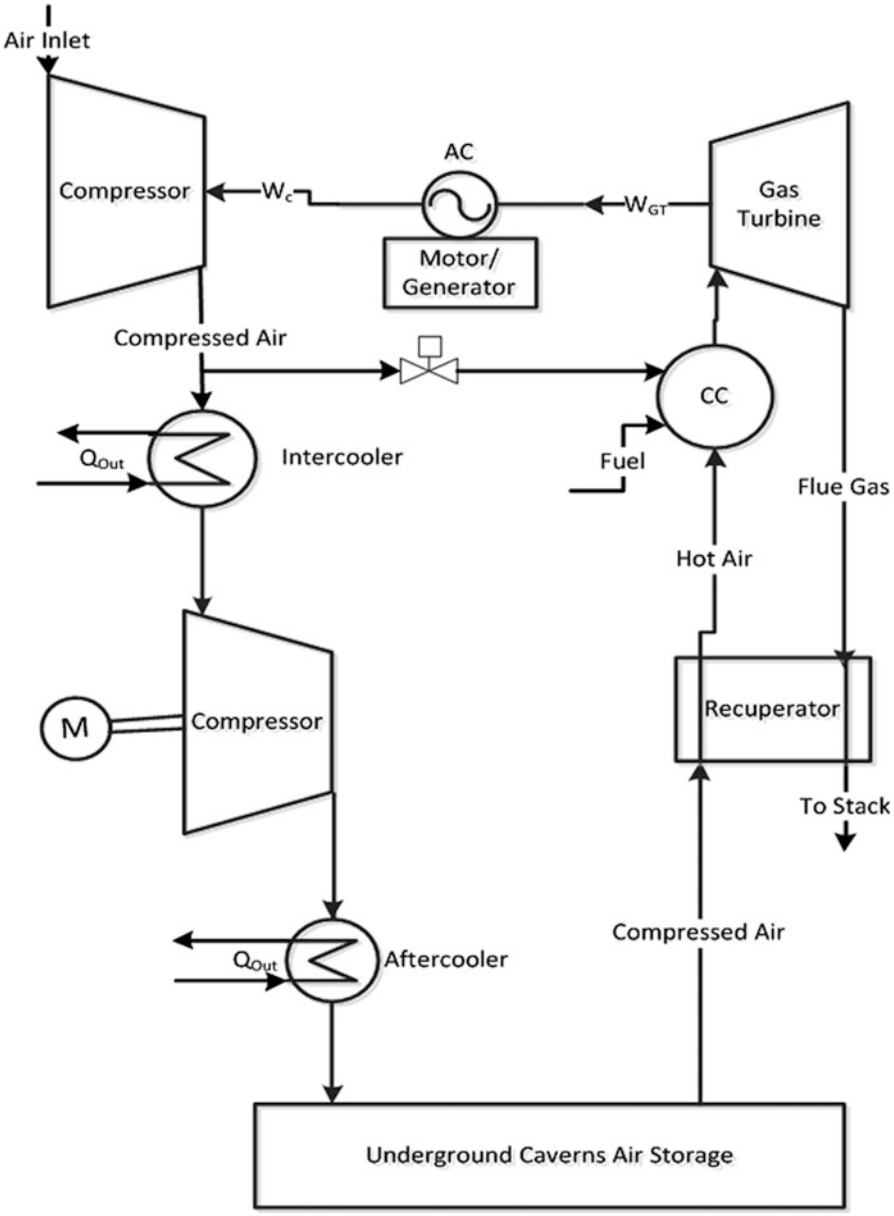

Fig. 41.15 Simplified schematic of compressed air energy storage system with its components

The SOFC-MGT cycle integrated with biomass gasification shown in Fig. 41.5 can take advantage of integration with other renewable energy resources and heat recovery technologies. There is a great need for drinking water in coastal areas, since most of these areas suffer from potable water shortages. Thermal desalination units can provide communities with healthy water, at reasonable prices. The energy

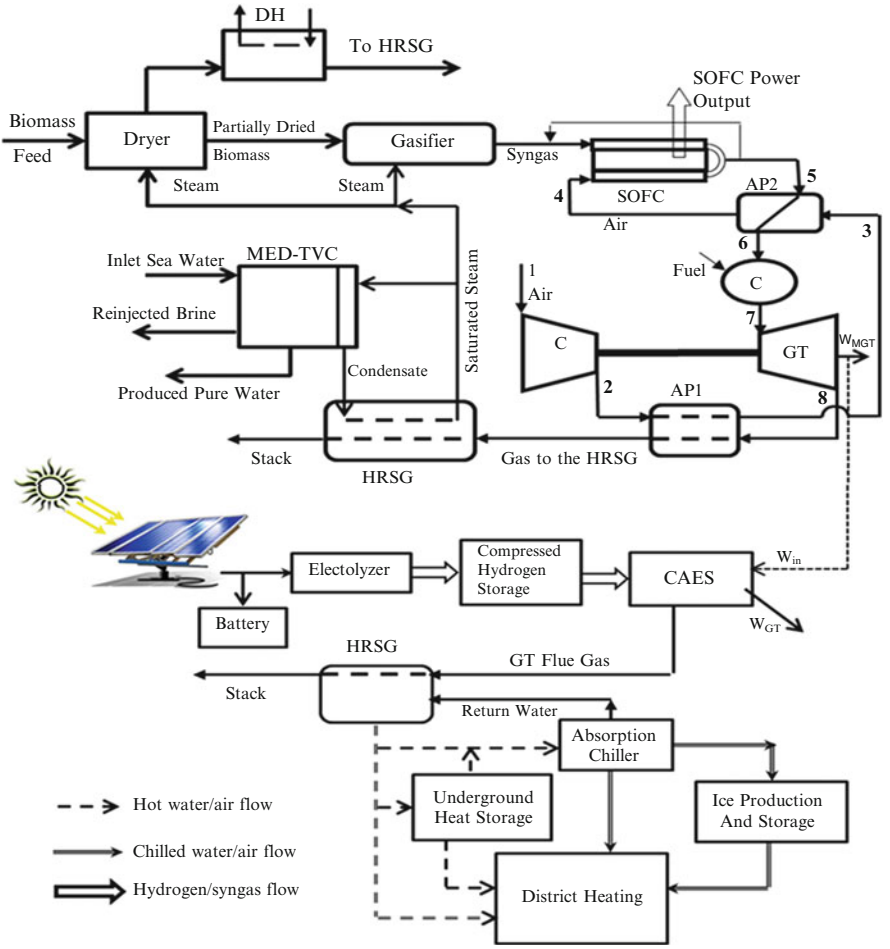

Fig. 41.16 Hybrid SOFC-micro gas turbine system with thermal desalination and energy storage options for coastal areas

requirement of thermal desalination systems can be met with any kind of available heat, e.g., waste heat from gas turbine exhaust gas. Hosseini et al. [21] proposed an integrated system containing a hybrid SOFC-MGT and a multi-effect desalination (MED) system. Along with power generation by the hybrid system, waste heat recovery from a micro gas turbine gives the opportunity to produce potable water.

In Fig. 41.16a schematic of the integrated system is shown [26]. To implement renewable energy resources, the integrated system is joined with a biomass gasification plant and a solar PV system. Energy storage options are included in the systems to enhance efficiency and power and heat reliability. The MGT flue gas (Point 8) is used to preheat the SOFC inlet air (AP1), and to produce saturated steam in the HRSG. The HRSG outlet steam enters the MED system in order to provide heat for pure water production, and to provide the gasification plant with the

required steam. During off-peak hours, the power output of the micro gas turbine is fed to the CAES system. While the gas turbine of the CAES system is in operation, it consumes the produced hydrogen in the solar PV-electrolyzer system as fuel. The gas turbine flue gas is fed to a heat recovery unit for enhanced energy utilization. The integrated system presented in Fig. 41.16 can supply a coastal area with electricity, drinking water, and thermal energy with the use of renewable energy resources. The development and implementation of such systems can reduce GHG emissions significantly.

41.5 Conclusions

Integrated renewable-based energy systems are developed with the purpose of reducing GHG emissions and mitigating global warming, and the role of IRESs in decreasing GHG emissions is reviewed here. Various types of renewable energy resources can be integrated in a system to provide the thermal and electrical energy of a house, a residential area, or a community. Also, the possibilities of implementation of these systems in residential and coastal areas are discussed by providing the results of energy and exergy analyses of two integrated systems, which utilize solar and biomass as the main sources of energy. The systems are compared with conventional power generation methods in terms of GHG emissions, demonstrating that the hybrid PV-FC system has zero carbon dioxide emissions during its operation while the integrated biomass-SOFC-MGT system emits less CO_2 than a fossil power plant. The integrated system configurations depend on the energy source and the demand profiles. Although these systems are not economically available today, several cases of their implementation are reported. Moreover, results of modeling and analyses of IRESs are presented in literature.

References

1. Boden TA, Marland G, Andres RJ (2010) Global, regional, and national fossil-fuel CO2 emissions. Carbon Dioxide Information Analysis Center, Oak Ridge National Laboratory, U.S. Department of Energy, Oak Ridge, TN, USA. doi:10.3334/CDIAC/00001_V2010
2. LeMar P (2002) Integrated energy systems (IES) for buildings: a market assessment. September 2002, Prepared by Resource Dynamics Corporation, Contract No. DE-AC05-00OR22725
3. Hosseini M, Rosen MA, Dincer I (2011) Hybrid solar-fuel cell CHP systems for residential applications. In: World engineering convention, Geneva, 4–9 Sept 2011
4. Hosseini M, Dincer I, Rosen MA (2013) Hybrid solar-fuel cell CHP systems for residential applications: energy and exergy analyses. J Power Sources 221:372–380
5. Hosseini M, Dincer I, Rosen MA (2012) Steam and air fed biomass gasification: comparisons based on energy and exergy. Int J Hydrogen Energy 37:16446–16452
6. Hosseini M, Dincer I, Rosen MA (2012) Thermodynamic analysis of a cycle integrating a solid oxide fuel cell and micro gas turbine with biomass gasification. 11th International conference on sustainable energy technologies (SET 2012), Vancouver, Canada, 2–5 Sept 2012

7. Hosseini M, Dincer I, Naterer GF, Rosen MA (2012) Thermodynamic analysis of filling compressed gaseous hydrogen storage tanks. Int J Hydrogen Energy 37:5063–5071
8. Gibson TL, Kelly NA (2008) Optimization of solar powered hydrogen production using photovoltaic electrolysis devices. Int J Hydrogen Energy 33:5931–5940
9. Largose J, Simoe MG, Miraoui A, Costerg P (2008) Energy cost analysis of a solar-hydrogen hybrid energy system for stand-aloneapplications. Int J Hydrogen Energy 33:2871–2879
10. Pregger T, Graf D, Krewitt W, Sattler C, Roeb M (2009) Prospects of solar thermal hydrogen production processes. Int J Hydrogen Energy 34:4256–4267
11. Hosseini M, Ziabasharhagh M (2010) Energy and exergy analysis of a residential SOFC-GT/absorption chiller system. Proc. ECOS 2010, 14–17 June, Lausanne, 5:411–418
12. Akkaya AV, Sahin B, Erdem HH (2008) An analysis of SOFC/GT CHP system based on exergetic performance criteria. Int J Hydrogen Energy 33:2566–2577
13. Hawkes AD, Aguiar P, Croxford B, Leach MA, Adjiman CS, Brandon NP (2007) Solid oxide fuel cell micro combined heat and power system operating strategy: options for provision of residential space and water heating. J Power Sources 164:260–271
14. Velumani S, Guzman CE, Peniche R, Vega R (2009) Proposal of a hybrid CHP system: SOFC/microturbine/absorption chiller. Int J Energy Research 34:1088–1095
15. Hartkopf VH, Archer D, Brahme R, Yin H (2003) A fuel cell based energy supply system for a multi-purpose building. 14th National conference of the Facility Management Association of Australia limited (FMA Australia), Sydney, Australia, 7–9 May, 2003
16. Paepe MD, Dherdt P, Mertens D (2006) Micro-CHP systems for residential applications. Energy Conversion and Management 47:3435–3446
17. Cohce MK, Dincer I, Rosen MA (2010) Thermodynamic analysis of hydrogen production from biomass gasification. Int J Hydrogen Energy 35:4970–4980
18. Abuadala A, Dincer I, Naterer GF (2010) Exergy analysis of hydrogen production from biomass gasification. Int J Hydrogen Energy 35:4981–4990
19. Basu P (2010) Design of biomass gasifiers. In: Biomass gasification and pyrolysis. Elsevier, Kidlington
20. Abudala A, Dincer I (2012) A review on biomass-based hydrogen production and potential applications. Int J Energy Res. doi:10.1002/er.1939
21. Hosseini M, Dincer I, Avval HB, Ahmadi P, Ziabasharhagh M (2011) Thermodynamic analysis of SOFC-MGT systems for desalination purposes. Int J Energy Res. doi:10.1002/er.1945
22. Colpan CO, Dincer I, Hamdullahpur F (2007) Thermodynamic modeling of direct internal reforming solid oxide fuel cells operating with syngas. Int J Hydrogen Energy 32:787–795
23. Syed AM, Fung AS, Ugursal VI, Taherian H (2009) Analysis of PV/wind potential in the Canadian residential sector, through high-resolution building energy simulation. Int J Energy Res 33:342–357
24. Calderon M, Calderon AJ, Ramiro A, Gonzalez JF, Gonzalez I (2011) Evaluation of a hybrid photovoltaic-wind system with hydrogen storage performance using exergy analysis. Int J Hydrogen Energy 36:5751–5762
25. Greenblatt JB, Succar S, Denkenberger DC, Williams RH, Socolow RH (2007) Baseload wind energy: modeling the competition between gas turbines and compressed air energy storage for supplemental generation. Energy Policy 35:1474–1492
26. Hosseini M, Dincer I, Rosen MA (2011) Investigation of energy storage options for sustainable energy systems, PhD candidacy exam report, University of Ontario Institute of Technology